

Site selectivity in chemisorption of C on Pd(211)Sergey Stolbov,¹ Faisal Mehmood,¹ Talat S. Rahman,^{1,2} Matti Alatalo,³ Ilja Makkonen,⁴ and Petri Salo⁴¹*Department of Physics, Cardwell Hall, Kansas State University, Manhattan, Kansas 66506, USA*²*Abteilung Physikalische Chemie, Fritz-Haber-Institut der Max-Planck-Gesellschaft, Faradayweg 4-6, D-14295 Berlin, Germany*³*Department of Electrical Engineering, Lappeenranta University of Technology, FIN-53851 Lappeenranta, Finland*⁴*Laboratory of Physics, Helsinki University of Technology, FIN-02015 HUT, Finland*

(Received 26 December 2003; revised manuscript received 8 July 2004; published 26 October 2004)

Results of *ab initio* electronic structure calculations of C on Pd(211), a vicinal of Pd(111), show a hierarchy of adsorption sites with adsorption energy ranging from -8.21 to -5.46 eV (0.33 ML coverage) and scaling almost linearly with the effective coordination at the site. In the most preferred site, C atoms sit almost under the Pd step atoms and influence drastically multilayer relaxations and surface registry of Pd(211). The adsorption energy at this site is -9.10 eV for 0.17 ML coverage. The local densities of electronic states indicate strong hybridization between C *p* states and neighboring Pd *d* states leading to the formation of strong covalent C—Pd bonds. The depletion of the electronic density of states of the Pd surface atoms at the Fermi level suggests a poisoning effect of C which is found to be coverage dependent. We compare the changes in the electronic structure of Pd(211) on C adsorption with those on S adsorption.

DOI: 10.1103/PhysRevB.70.155410

PACS number(s): 73.20.—r

I. INTRODUCTION

Elementary steps in heterogeneous catalysis such as molecular adsorption and dissociation proceed through the reorganization of chemical bonds between reactants and the surface. At the same time, the surface either by itself, or in the presence of adsorbed species, may undergo lattice relaxations which in turn affect surface chemical bonding. An understanding of microscopic mechanisms of heterogeneous catalysis thus requires careful consideration of both the electronic and the geometric structure of catalyst surfaces. Since several competing factors may influence a chemical reaction, the strategy over the years has been to isolate the role of the geometrical, structural and compositional characteristics that are expected to be important. Among these, the influence of steps^{1–8} and impurities^{9,10} on the electronic and geometric structure of transition metal surfaces has been of great interest. This is not surprising since steps are omnipresent, even under reasonably controlled conditions. Furthermore, in a number of laboratory experiments steps have been identified as the reactive sites for processes such as molecular dissociation^{2,3,11} and other reactions.¹² The specific role of step atoms in a chemical reaction may, however, be more complex¹³ and may not always lead to enhanced reactivity.¹⁴ Similarly, it is not difficult to imagine the important role of impurities in changing the local or extended electronic structure of transition metal surfaces and thereby controlling the outcome of a chemical reaction. In particular, adsorbed species such as C, S, and N have been the subject of much discussion in the literature on chemisorption and chemical reactivity. Several experimental studies have focussed on the poisoning effect of these adsorbates,^{15–20} although open questions remain about the impact of C on chemical reactivity.²¹ From a theoretical stand point, the prior question is how to measure the poisoning or the promotion of chemical reactivity. In one of the first such studies, Feibelman and Hamann⁹ proposed that the electronic structure of Rh(001) was “poisoned” by the adsorption of S because of the deple-

tion of the density of states at the Fermi level which extended to a number of Rh neighbors. Theoretical calculations for S on Pd(100) (Ref. 10) also showed a reduction of the density of states at the Fermi level resulting from a strong hybridization of the *p* states of S with the *d* states of Pd. More recent studies of Makkonen *et al.*²² for S adsorption on a set of stepped Pd surfaces, which are vicinal to Pd(111) and Pd(110), also show a depletion of the density of states of neighboring Pd atoms on S adsorption, but for these vicinal surfaces the effect is site selectivity and dependent on the surface geometry and local coordination. The effect of S adsorption on multilayer relaxation and surface registry of the Pd surfaces was also found to be remarkable and led to site specific modification in the surface electronic structure. In the present work, we have investigated the effect of C adsorption on Pd(211), for several reasons. First, C is known to exist as an impurity on surfaces,^{18,23} and its small size and abundance makes it a challenge for experimentalists to free their surface of it. Assumptions have been made that it acts as a poison,^{18,20} but some debate continues. Second, CO oxidation is one of the most important processes in which the blocking of reactive sites by C may be an important issue. Third, a comparative study of the effect of C and S on a stepped transition metal surface would provide a measure of the strength of the impurity—substrate bond and its impact on the surface electronic structure. Finally, a systematic study of C adsorption on stepped surfaces is a step towards understanding the role of undercoordinated sites in chemical reactivity. Since the nonequivalent atoms on a vicinal surface, in the presence of an adsorbate, account for a complex and inhomogeneous system, these studies are expected to have implications also for the characteristics of nanoparticles which contain a range of undercoordinated sites in complex environments.

In what follows we provide a comprehensive description of the geometric and electronic structure of C adsorbed on Pd(211). Our study includes a detailed examination of local properties such as atomic relaxation, local densities of elec-

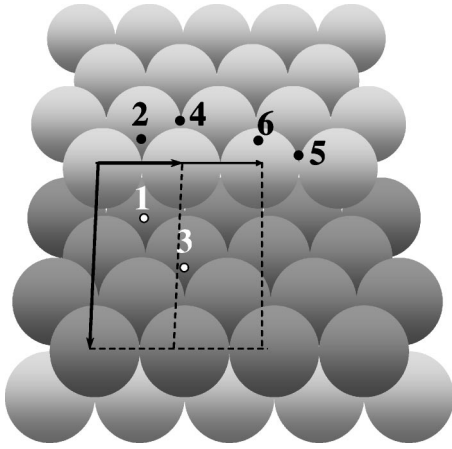


FIG. 1. Adsorption sites in Pd(211) considered in this paper.

tronic states, and charge distribution at and near the preferred adsorption sites. These characteristics are compared with those for S adsorption on Pd(211) and those for clean Pd(211) to observe trends in the behavior. The effect of the C coverage on the properties is also examined. Some details of the computational technique are summarized in Sec. II, followed by results and discussions in Sec. III, and conclusions in Sec. IV.

II. COMPUTATIONAL DETAILS

Calculations presented in this paper were performed within the density functional theory with the generalized-gradient approximation (GGA) for the exchange-correlation functional.²⁴ The Pd(211) surface was modelled by an orthorhombic supercell consisting of a 17 layer slab and 11 Å of vacuum. The (211) surface of fcc metals consists of three atomic chains forming (111) terraces separated by monoatomic steps of the (100) orientation. Throughout the paper we use the following notation for these chains: SC (step chain) for step atoms, TC (terrace chain) for the chain running through the middle of the terrace, CC (corner chain) for the chain located between TC and SC, and BNN (bulk nearest neighbor) located just beneath SC.

Two coverages of adsorbate corresponding roughly to 0.33 and 0.17 ML are considered. For the former case, this implies the inclusion of one C atom per three Pd atoms (SC, TC, or CC). For the latter case, the unit cell contains one C atom per six Pd surface atoms. The two-dimensional unit cells for both cases are shown in Fig. 1. For the 0.33 ML coverage the unit cell has surface translation vectors $a = a_{\text{blk}}/\sqrt{2}$ and $b = a_{\text{blk}}\sqrt{3}$, where a_{blk} denotes the bulk lattice parameter. For the case of the 0.17 ML coverage, the b vector is doubled. For the higher coverage, the calculations have been performed for six different adsorption sites with C atom placed on one side of the Pd slab at each of the positions shown in Fig. 1. For the system with 0.17 ML coverage, we have calculated the geometric and electronic structure only for the most preferred adsorption site (the site 1 in Fig. 1) for brevity.

The surface relaxations and adsorption energies E_{ad} have

been calculated using the Vienna *ab initio* simulation package (VASP)²⁵ which is based on the plane-wave pseudopotential (PWPP) method.²⁶ The ultrasoft pseudopotentials^{27,28} were used for C and Pd. We set cutoff energies for the plane-wave expansion of 199 eV for the clean Pd(211) and 287 eV for C/Pd(211) systems. A $10 \times 5 \times 1$ Monkhorst-Pack k -point mesh was used to sample the Brillouin zone.²⁹ During the lattice relaxation, all atoms were allowed to move along the z axis (normal to the surface) and along the direction normal to the step within the surface plane (y axis). For the 0.17 ML coverage relaxation along the steps was also allowed. The structures were relaxed until the forces acting on each atom converged better than 0.02 eV/Å.

A full analysis of the electronic structure, which includes calculations of the local density of states (LDOS), valence charge density and local charges of the systems, were performed using a full-potential linear-augmented plane-wave (FLAPW) method³¹ as embodied in the WIEN2K code.³⁰ For the calculation of the local properties of interest, the FLAPW method appears to be more appropriate as compared to the one based on the plane-wave expansion for wave functions. Relaxed structures obtained from calculations using the VASP code were used as input for the WIEN2K code which further refined the geometries in a few ionic iterations. In the FLAPW method, the LDOS and local charges are calculated through integration over muffin-tin (MT) spheres of radius R_{MT} . To analyze the effect of adsorbate on these specific quantities the set of R_{MT} for Pd atoms should be chosen to be the same for both the clean and the adsorbate covered Pd(211). Ideally R_{MT} should be as large as possible without causing the MT spheres to overlap. For bulk Pd atoms, a choice of $R_{\text{MT}} = 1.22$ Å was found to be optimal. However, for the Pd atoms (SC, CC, and BNN) with direct bonds to C, $R_{\text{MT}} = 1.005$ Å provided more compatibility with the shorter C—Pd bond lengths. For C atoms, $R_{\text{MT}} = 0.926$ Å was found to be appropriate. In order to include a reasonably large number of plane waves ($RK_{\text{max}} = 7$) with the reduced R_{MT} 's for the surface atoms, we used basis sets of 2937 and 3500 LAPW's for Pd(211) and C/Pd(211), respectively. The calculations were performed for the $7 \times 3 \times 1$ k -point mesh in the Brillouin zone. Earlier calculations of S on Pd(211)²² were performed using only the plane wave basis (as in VASP). Since our intention in this paper is to compare the effects of C adsorption with those of S, we have extended the FLAPW calculations to S/Pd(211) system. The R_{MT} for S was taken to be 1.005 Å and the basis set consisted of 2913 LAPW's.

III. RESULTS AND DISCUSSION

A. Adsorption energies and surface relaxation

In this section we first present the results for the adsorption energies of C on Pd(211) whose hierarchy is indicative of a site selectivity. We also analyze the impact that the chemisorption of C has on multilayer relaxation and in-plane registry of the Pd atoms. This is followed by a detailed analysis of the electronic structure of the chemisorbed system with particular emphasis on the distribution of electronic-charge density and local charges, the LDOS, and

TABLE I. C and S adsorption energies (eV) at various sites on Pd(211).

Site	C(0.33 ML)	C(0.17 ML)	S(0.33 ML)	S(0.17 ML)
1	-8.21	-9.10	-4.44	-5.39
2	-7.98		-4.30	
3	-7.51		-4.31	
4	-7.30		-4.36	
5	-6.22		-3.73	
6	-5.46		-3.33	

the nature of the bonds between the C atoms and their nearest neighbor Pd atoms. To compare the effect of C and S as adsorbates on Pd(211), some results for S have been taken from Ref. 22, while the others have been calculated.

For C adsorption (0.33 ML coverage) on Pd(211) six adsorption sites with energy ranging from -8.21 to -5.46 eV are found. The approximate positions of these sites are illustrated in Fig. 1 and the corresponding adsorption energies (E_{ad}) are summarized in Table I. The most preferred site, labeled 1, is just below the step atoms and has an effective coordination of 5, as it binds with two SC, two CC, and one BNN atoms. Very close in adsorption energy (-7.98 eV) is the site 2 in which the C atom sits at the threefold hcp hollow site, at the step edge, and obtains coordination with four nearby Pd atoms. Next in hierarchy is the site 3 on the threefold hcp hollow site on the terrace with $E_{ad} = -7.51$ eV and the coordination 4. As with site 2, site 4 is at the top of the step, but at the three-fold fcc site and hence has a coordination of 3. The bridge site (labeled 5) between the step atoms also offers $E_{ad} = -6.22$ eV and the coordination 2, while the lowest E_{ad} is at the site 6 which is on-top of the Pd step atom. For the most preferred site (site 1), our calculations show an adsorption energy of -9.10 eV for the lower C coverage (0.17 ML).

In Fig. 2 we find a correlation between the adsorption energy E_{ad} and the number of adsorbate-substrate bonds formed for the six C adsorption sites. This is an expected

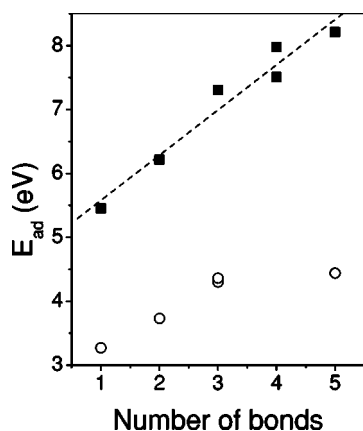


FIG. 2. Correlation between the C (bold squares) and S (empty circles) adsorption energy and the number of the adsorbate-Pd bonds extracted from the calculations performed for the adsorption sites shown in Fig. 1.

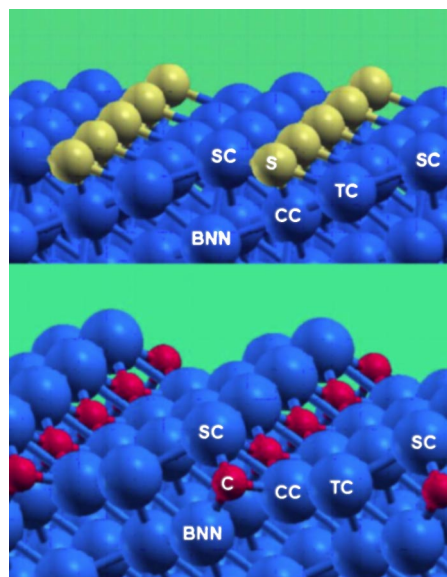


FIG. 3. (Color online) Geometric structures of $S_{0.33}/Pd(211)$ and $C_{0.33}/Pd(211)$.

result: the more bonds, the higher is the adsorption energy. For C/Pd(211), E_{ad} scales almost linearly with the effective coordination at the site. In Table I and Fig. 2 we have also included the results for S adsorption from Ref. 22. The adsorption energy is found to be much higher for C than that for S for the sites studied. Note that although the approximate location of the sites for C and S is the same, C penetrates much closer to the surface atoms than S. For the most preferred site, the coordinates of the C and S atoms, measured in Å from the nearest step atom, are found to be $(-1.4, -1.02, -1.04)$ and $(-1.39, -2.08, 0.18)$. A perspective for this adsorption site shown in Fig. 3 illustrates the difference in the geometry for the C and S atoms on this surface. Carbon, being smaller in size, goes deeper under the step than sulfur does. The differences in the exact location of the C and S atoms is also reflected in the plot E_{ad} versus coordination in Fig. 2, in which the scaling with coordination for S adsorption holds only for the low coordination sites. In fact, in the case of S, the adsorption energy for the sites 2, 3, and 4 is almost the same, and for the site 1 it is only slightly higher, while the differences are larger for C adsorption.

The presence of the C atoms that close to the Pd surface atoms has drastic effects on the surface geometry. Both interlayer relaxations and in-plane registry are affected by C chemisorption. In Table II, we have summarized the calculated percentage change in the interlayer spacing $d_{i,i+1}$, where layers i are defined with respect to the [211] planes, as usual. For comparison we have included in Table II the case of C adsorption in the site 1 (C1) and in the site 2 (C2). The changes in the multilayer relaxation for clean Pd(211) and in the presence of S in the site 1 from Ref. 22 are also displayed in Table II. The most noticeable change is the outward relaxation of the step atom for C adsorption near it. Since C penetrates into the Pd surface, the step atoms accommodate it by moving outwards. The TC and the CC atoms behave understandably differently for C adsorption in the sites 1 and 2. Since the TC atom does not form a strong bond with the

TABLE II. Multilayer relaxation (%).

$d_{i,i+1}$	C1/Pd(211)	C2/Pd(211)	Pd(211)	S1/Pd(211)
$d_{1,2}$	22.6	30.8	-12.3	-13.2
$d_{2,3}$	-14.9	27.5	-13.0	31.4
$d_{3,4}$	23.6	-16.8	17.4	-10.0
$d_{4,5}$	-4.3	12.0	-6.1	2.3
$d_{5,6}$	3.2	3.6	-2.0	4.0
$d_{6,7}$	2.8	-5.1	3.6	-2.2
$d_{7,8}$	-5.7	4.0	-2.7	2.4
$d_{8,9}$	4.5	0.9	0.0	2.6
$d_{9,10}$	0.5	-1.1	0.0	0.0

carbon atom in the site 1, its bond with the CC atom (d_{23}) remains almost the same as that on clean Pd(211). On the other hand, C in the site 2 forms a strong bond with the TC atom causing them to move outwards just as the neighboring step atoms do, resulting in a strong outward relaxation of d_{23} . The effect of C adsorption on the relaxation of d_{34} is also very remarkable. In the site 1, the carbon atom pushes the CC atom outwards to make room for itself, while in the site 2 it has to push it down for the same purpose, resulting in relaxations which are distinctly different from those on clean Pd(211), for both adsorption sites. In contrast, S adsorption in the site 1 (see Fig. 3) does not impact the relaxation of the step atoms, rather the effect is mostly on the relaxations of the TC and the CC atoms. These variations in the multilayer relaxations of Pd(211) induced by the C and S atoms will be further reflected in the changes in the local electronic structure of Pd(211), as seen below.

In Table III, we have assembled the registry of the Pd atoms in the surface layers. Here Δy_i represents the change of the location of the Pd atom in the layer i , along the normal to the step, in the surface plane. In our notation, the step atoms lie along the x axis. Here again there is a remarkable difference in the cases considered. With C in the site 1, the registry of both TC and CC atoms are affected in a shearing manner, while S appears to push the step atoms somewhat inwards. The most significant effect on surface registry appears for C adsorption in the site 2 in which the step atoms move inwards by 0.58 Å. For brevity, we have not included in Tables II and III the results for the other four adsorption sites, which follow the same rationalization as the ones presented.

TABLE III. Surface registry (Å).

	C1/Pd(211)	C2/Pd(211)	S1/Pd(211)
Δy_1	-0.07	-0.58	-0.13
Δy_2	0.12	0.15	-0.06
Δy_3	-0.15	0.0	0.0
Δy_4	-0.04	0.07	0.06
Δy_5	0.0	0.05	-0.03
Δy_6	-0.02	0.06	0.0

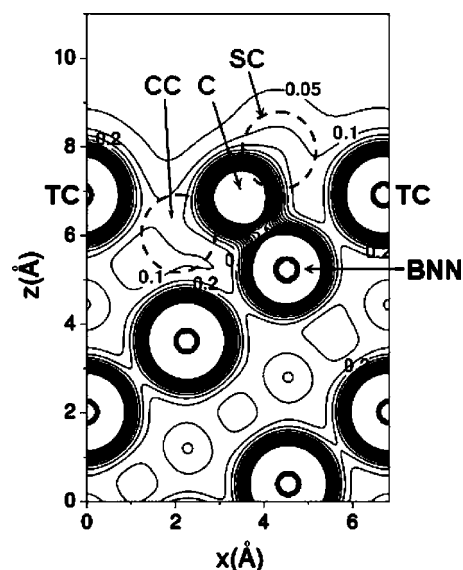


FIG. 4. Valence electronic density calculated for $C_{0.33}/Pd(211)$ with the adsorption site 1 and plotted along the plane normal to the surface and including C and BNN sites.

B. Electronic structure

Using the FLAPW method, we have calculated the charge densities along certain planes which include the main bonds formed between the adsorbate and Pd atoms in Pd(211). Since there is a significant difference between the charge density distribution for the C and S adsorption cases, we present each in Figs. 4 and 5, respectively, to illustrate the point. Because of its small size, carbon is located below the SC and TC layers, close to the BNN atom, forming a strong covalent bond with the BNN atom seen in Fig. 4 as a charge density bridge. In contrast, S is located above the surface close to the TC atom (see Fig. 6) forming a weak covalent bond with the TC atom, and no noticeable bond with the BNN atom. A plot of the charge density along the plane containing the SC and CC atoms, and carbon atoms (Fig. 6) shows that carbon also forms strong covalent bonds with these Pd atoms. More detailed information about chemical bonding can be obtained from plots showing the difference $\delta\rho(r)$ between the self-consistent charge density of the system and the sum of the densities of free atoms placed at the corresponding sites. Such plots reflect the charge redistribution caused by the chemical bonding. Shown in Figs. 7 and 8 is $\delta\rho(r)$ calculated for C/Pd(211) and S/Pd(211), respectively, along the (010) plane which includes the centers of C(S), the TC and the BNN atoms. It is seen from the figures that bulklike Pd atoms (located not too close to the surface) donate some electronic density to interstitial region to build comparatively weak Pd—Pd covalent bonds. Both C and S accept a significant amount of the electronic charge from neighboring Pd, making the C—Pd and S—Pd bonds essentially ionic. However, a distinct electronic-density bridge between the C and the BNN atoms is also present in Fig. 7, reflecting strong C—Pd covalent bonding. In contrast, no significant electron-density bridge is seen between S and the TC atom in Fig. 8. Thus, the S—Pd bonding in S/Pd(211) is

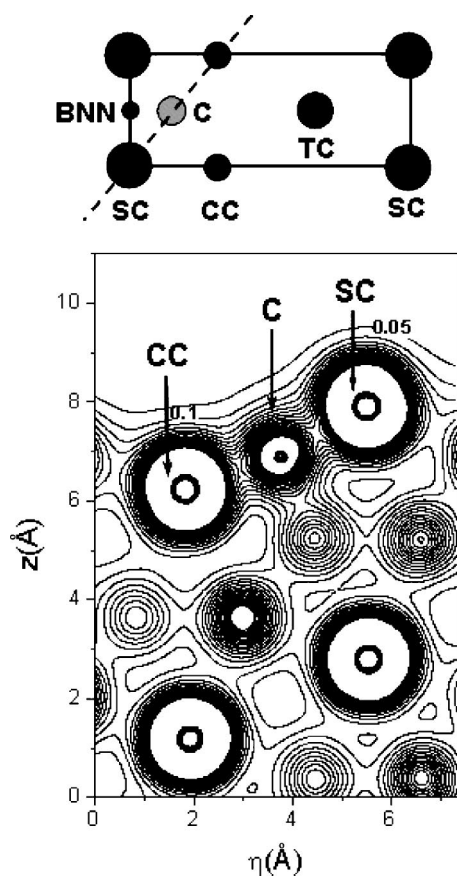


FIG. 5. The same as in Fig. 4, but plotted along the plane normal to the surface and connecting the SC and CC sites. The nucleus of the C atom is located slightly out of the plane.

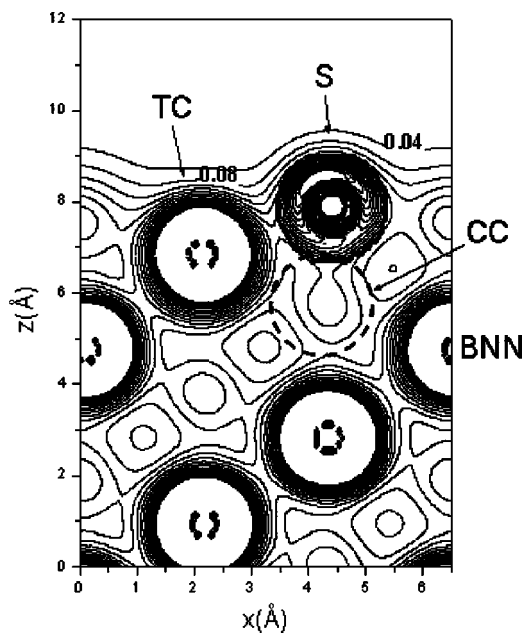


FIG. 6. Valence electronic density calculated for $S_{0.33}/Pd(211)$ with the adsorption site 1 and plotted along the plane normal to the surface and including S and BNN sites.

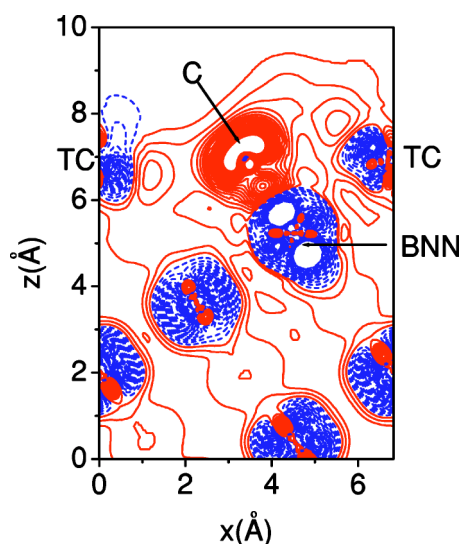


FIG. 7. (Color online) Electronic density redistribution in $C_{0.33}/Pd(211)$ with respect to the sum of densities of non-interacting atoms. Solid red and dashed blue lines denote the positive and negative deviation, respectively.

mostly ionic with a small covalent contribution, whereas C and the BNN atom form a mixed ionic-covalent bond. An analysis of the charge density and $\delta\rho(r)$ plotted along other planes indicates that the C—SC, C—CC, S—SC, and S—CC covalent bridges are also formed, and again, the C—Pd bridges in C/Pd(211) are much stronger than the S—Pd bonds in S/Pd(211).

While the above plots of the charge density distribution have provided a good insight into the extent of the electronic overlap between the different atoms and the nature of the bonding between the adsorbate and Pd atoms, they do not

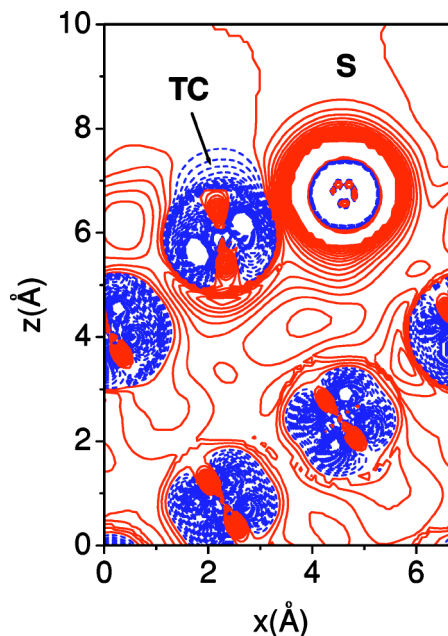


FIG. 8. (Color online) The same as in Fig. 7, but for $S_{0.33}/Pd(211)$.

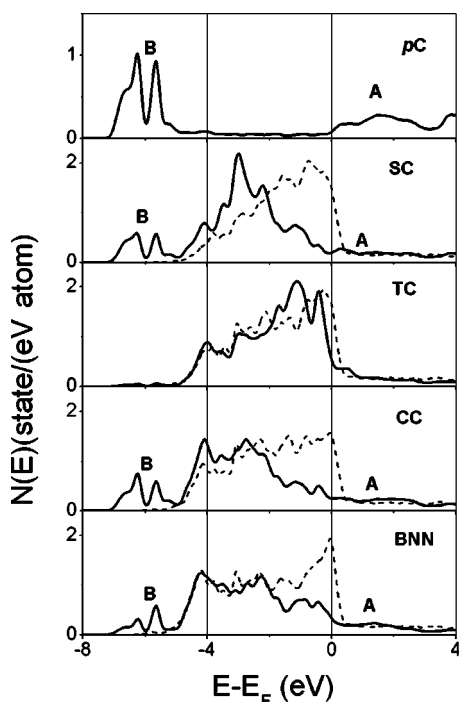


FIG. 9. Local densities of C and Pd electronic states calculated for $C_{0.33}/Pd(211)$ with the adsorption site 1 (solid line) and for clean Pd(211) (dashed line).

address the issue of reactivity of the surface. For this we turn to the calculated local properties. Shown in Fig. 9 are LDOS calculated for C on Pd(211) in the adsorption site 1. The density of C p states is found to be split forming the bonding (B) and antibonding (A) subbands with the SC, CC, and BNN atoms. Since the antibonding states are not occupied when C adsorbs on Pd(211) and the splitting between bonding and antibonding subbands is large (7–8 eV), strong covalent bonds are expected between carbon and its neighboring Pd atoms: SC, CC, and BNN. Similar plot of the LDOS for the S atom (see Fig. 10) shows that it forms bonding and antibonding subbands with the SC, TC, and CC atoms and does not form such bonds with the BNN atom. This difference between LDOS of C/Pd(211) and S/Pd(211) reflects the difference in their charge density distribution discussed above.

To examine the effect of coverage, we present in Figs. 11 and 12 the LDOS calculated for 0.17 ML coverage of C and S on Pd(211) [$C_{0.17}/Pd(211)$ and $S_{0.17}/Pd(211)$], respectively. On comparing these plots with those shown in Figs. 9 and 10, we find that as the coverage decreases the effect of the adsorbates on the LDOS of the neighboring surface atoms becomes weaker. This is not surprising since at 0.17 ML coverage each SC or CC atom has one neighboring adsorbate atoms, while at 0.33 ML it has two such atoms. However, even at the lower coverage the band splitting caused by the adsorbate is still substantial for the SC and CC atoms, especially in the case of C adsorption.

The formation of the bonding and anti-bonding subbands causes a significant reduction of the density of electronic states at the Fermi level [$N(E_F)$]. The values of local $N(E_F)$ for surface Pd atoms in Pd(211) (clean and in the presence of

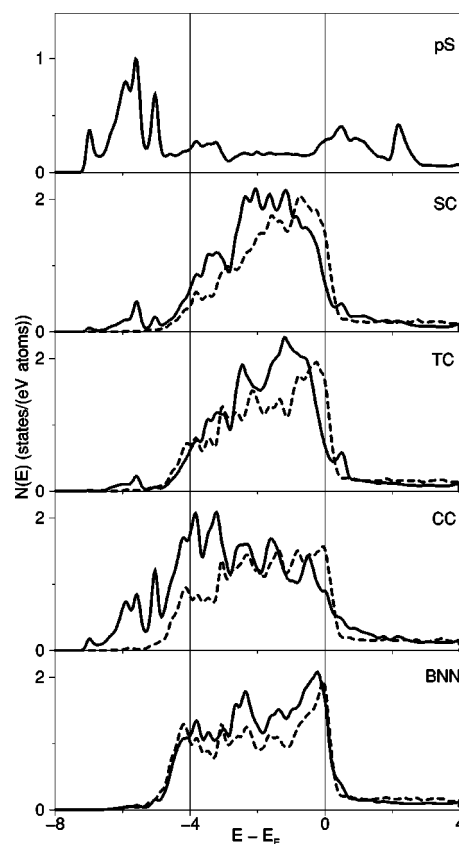


FIG. 10. The same as in Fig. 9, but for $S_{0.33}/Pd(211)$.

the C and S atoms) are listed in Table IV. One can see that for the 0.33 ML coverage the presence of the adsorbate leads to dramatic decrease in $N(E_F)$ for all surface atoms, and the effect is especially strong for C/Pd(211). For the 0.17 ML coverage the effect is smaller, however, it is still substantial:

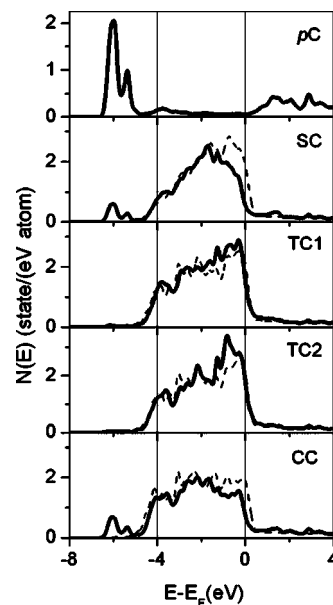


FIG. 11. Local densities of C and Pd electronic states calculated for $C_{0.17}/Pd(211)$ with the adsorption site 1 (solid line) and for clean Pd(211) (dashed line).

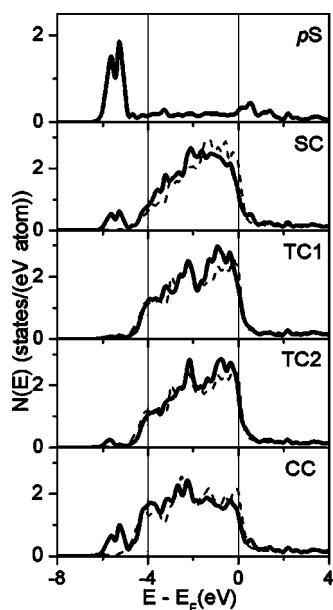


FIG. 12. The same as in Fig. 11, but for $S_{0.17}/\text{Pd}(211)$.

C adsorption reduces $N(E_F)$ at the neighboring SC and CC atoms by 3–4 times.

If we recall that in experiments S poisons reactions on Pd, our results for S adsorption support the proposition that a depletion of electronic states around E_F may cause a decrease in surface reactivity. Even at a lower coverage, each adsorbate has four Pd neighbors in the surface (two SC and two CC atoms) whose $N(E_F)$ is substantially reduced.

IV. CONCLUSIONS

In this work we have examined the changes in the geometric and electronic structure of Pd(211) induced by the adsorption of a third of a monolayer of C atoms. A hierarchy of six adsorption sites is found for which the adsorption energy ranges from -8.21 to -5.46 eV. The changes in the

TABLE IV. Local densities of electronic states at the Fermi level (eV atom) (Ref. 1) calculated for the Pd surface atoms in Pd(211), C/Pd(211), and S/Pd(211). Two numbers shown for TC and BNN for the low coverage systems correspond to nonequivalent atoms.

	SC	TC	CC	BNN
$C_{0.33}/\text{Pd}(211)$	0.20	0.53	0.25	0.33
$C_{0.17}/\text{Pd}(211)$	0.55	1.53(1.77)	0.74	0.92(1.95)
Pd(211)	2.21	2.30	2.19	2.37
$S_{0.33}/\text{Pd}(211)$	0.72	0.67	0.87	1.73
$S_{0.17}/\text{Pd}(211)$	1.14	1.59(1.62)	1.25	2.09(2.15)

local electronic structure and in the multilayer relaxation and surface registry patterns are found to be dramatic and site selective. In the most preferable adsorption site the C atoms are found to occupy positions almost under the step atoms thus forming strong bonds with five Pd atoms, including one in the bulk material (BNN). From the hybridization of the C p and Pd d states and estimates of the local charge density distributions the C—Pd bonds are found to be covalent, while S atoms similarly adsorbed lead to S—Pd bonds that are mostly ionic. Both C and S atoms lead to a depletion of the local electronic density of states near the Fermi level, indicating a poisoning effect. It would be interesting to have experimental data on two main aspects of the issues discussed here: the effect of C adsorption on multilayer relaxation and on the chemical reactivity of Pd(211). We hope our results here will motivate such experimental observations.

ACKNOWLEDGMENTS

T.S.R. thanks G. Rupprechter, H. Freund, and G. Ertl for helpful discussions. A grant from NCSA, Urbana, Illinois, was beneficial in providing computational resources. We acknowledge financial support from NSF, USA, under Grant No. CHE-0205064 and from the Academy of Science of Finland through its Center of Excellence program.

¹B. Hammer and J. K. Nørskov, Phys. Rev. Lett. **79**, 4441 (1997).

²P. Gambardella, Ž Žljivančanin, B. Hammer, M. Blanc, K. Kuhnke, and K. Kern, Phys. Rev. Lett. **87**, 056103 (2001).

³S. Dahl, A. Logadottir, R. C. Egeberg, J. H. Larsen, I. Chorkendorff, E. Törnqvist, and J. K. Nørskov, Phys. Rev. Lett. **83**, 1814 (1999).

⁴P. J. Feibelman, S. Esch, and T. Michely, Phys. Rev. Lett. **77**, 2257 (1996).

⁵B. Hammer, Phys. Rev. Lett. **83**, 3681 (1999).

⁶B. Hammer, J. Catal. **199**, 171 (2001).

⁷M. Mavrikakis, P. Stoltze, and J. K. Nørskov, Catal. Lett. **64**, 101 (2000).

⁸D. Loffreda, D. Simon, and P. Sautet, J. Catal. **213**, 211 (2003).

⁹P. J. Feibelman and D. R. Hamann, Phys. Rev. Lett. **52**, 61 (1984).

¹⁰S. Wilke and M. Scheffler, Phys. Rev. Lett. **76**, 3380 (1996).

¹¹T. Zambelli, J. Wintterlin, J. Trost, and G. Ertl, Science **273**, 1688 (1996).

¹²S. C. Creighan, R. J. Mukerji, A. S. Bolina, D. W. Lewis, and W. A. Brown, Catal. Lett. **88**, 39 (2003).

¹³M. Ikai and K. Tanaka, J. Chem. Phys. **110**, 7031 (1999).

¹⁴M. Hirsimäki and M. Valden, J. Chem. Phys. **114**, 2345 (2001).

¹⁵G. Comsa, R. David, and B. J. Schumacher, Surf. Sci. **95**, L210 (1980).

¹⁶K. D. Rendulic, G. Anger, and A. Winkler, Surf. Sci. **208**, 404 (1989).

¹⁷M. Kiskinova and Goldman, Surf. Sci. **108**, 64 (1981).

¹⁸S. M. Vesecky, D. R. Rainer, and D. W. Goodman, J. Vac. Sci. Technol. A **14**, 1457 (1996).

¹⁹M. Rutkowski, D. Wetzig, and H. Zacharias, Phys. Rev. Lett. **87**, 246101 (2001).

²⁰J. Libuda, I. Meusel, J. Hoffman, L. Piccolo, C. R. Henry, and

- H.-J. Freund, J. Chem. Phys. **114**, 4669 (2001).
- ²¹H. Freund (private communication).
- ²²I. Makkonen, P. Salo, M. Alatalo, and T. S. Rahman, Phys. Rev. B **67**, 165415 (2003).
- ²³V. Matolin, E. Gillet, and N. Kruse, Surf. Sci. **186**, L541 (1987).
- ²⁴J. P. Perdew and Y. Wang, Phys. Rev. B **45**, 13 244 (1992).
- ²⁵G. Kresse and J. Hafner, Phys. Rev. B **47**, 558 (1993).
- ²⁶M. C. Payne, M. P. Teter, D. C. Allan, T. A. Arias, and J. D. Joannopoulos, Rev. Mod. Phys. **64**, 1045 (1992).
- ²⁷D. Vanderbilt, Phys. Rev. B **41**, 7892 (1990).
- ²⁸G. Kresse and J. Hafner, J. Phys.: Condens. Matter **6**, 8245 (1994).
- ²⁹H. J. Monkhorst and J. D. Pack, Phys. Rev. B **13**, 5188 (1976).
- ³⁰P. Blaha, K. Schwarz, G. K. H. Madsen, D. Kvasnicka, and J. Luitz, WIEN2K, An Augmented Plane Wave + Local Orbitals Program for Calculating Crystal Properties (Karlheinz Schwarz, Technische Universität Wien, Austria, 2001).
- ³¹M. Weinert, E. Wimmer, and A. J. Freeman, Phys. Rev. B **26**, 4571 (1982); D. Singh, *Planewaves, Pseudopotentials and the LAPW Method* (Kluwer, Dordrecht, 1994).